Comparison of Open-Hole Tension Characteristics of High Strength Glass and Carbon Fibre-Reinforced Composite Materials

R.M. O'Higgins, M.A. Mccarthy, C.T. Mccarthy

Comparison of Open-Hole Tension Characteristics of High Strength Glass and Carbon Fibre-Reinforced Composite Materials

R.M. O'Higgins, M.A. McCarthy, C.T. McCarthy

PII: S0266-3538(08)00230-3
DOI: 10.1016/j.compscitech.2008.06.003
Reference: CSTE 4099

To appear in: *Composites Science and Technology*

Received Date: 17 January 2008
Revised Date: 27 May 2008
Accepted Date: 2 June 2008

Please cite this article as: O'Higgins, R.M., McCarthy, M.A., McCarthy, C.T., Comparison of Open-Hole Tension Characteristics of High Strength Glass and Carbon Fibre-Reinforced Composite Materials, *Composites Science and Technology* (2008), doi: 10.1016/j.compscitech.2008.06.003

Comparison of Open-Hole Tension Characteristics of High Strength Glass and Carbon Fibre-Reinforced Composite Materials

R.M. O'Higgins, M.A. McCarthy, C.T. McCarthy*

Composites Research Centre, Materials and Surface Science Institute, Department of Mechanical and Aeronautical Engineering, University of Limerick, Limerick, Ireland

Abstract

An experimental study was carried out to determine the open hole tension (OHT) characteristics of carbon fibre-reinforced plastic (CFRP) and high-strength S2-glass fibre-reinforced plastic (GFRP). Tests to failure and percentages of ultimate load were carried out and non-destructive techniques were used to map damage progression. It was found that the CFRP OHT specimens were stronger, while the GFRP OHT specimens had greater ultimate strain. However, damage progression mechanisms in the two material systems were very similar. This contrasts with previous findings on E-glass composites, indicating that S2-glass FRP notched failure behaviour is closer to a high performance CFRP. Higher levels of damage formation prior to failure were found to result in higher OHT strength (S_{OHT}). Blocked ply stacking sequences were found to give higher damage levels and S_{OHT} than sub-laminate level stacking sequences, and similar trends were found when laminate thickness was reduced. Non-linear transverse behaviour in GFRP resulted in lower levels of matrix cracking in OHT specimen 90º plies, compared to CFRP, providing a barrier to the growth of stress relieving axial splits in 0º plies.

Keywords: A. Carbon fibres; A. Glass fibres; B. Fracture, B. Mechanical properties

1. Introduction:

With the increasing cost of fuel and worries about the environmental impact of air travel, great efforts are being made to improve the efficiency of air transportation systems. One practical way of reducing structural weight and increasing payload efficiency is increasing the structural application of fibre-reinforced plastics (FRP), which offer improved specific properties compared to traditional metallic materials and allow more efficient manufacturing processes. It is estimated that a weight reduction of 1kg on an aircraft

* Corresponding author. Tel.:+353-61-234334; fax: +353-61-202944. *E-mail address:* conor.mccarthy@ul.ie (C.T. McCarthy)

equivalent in size to an Airbus A320 saves over 2,900 litres of fuel per year [1]. Generally, carbon fibre-reinforced plastics (CFRP) have been the composite material of choice for use in primary structures due to their high specific strength and modulus. As such, a considerable literature exists on the damage characteristics of notched CFRP laminates [2-17].

It has been widely reported that notch tip damage prior to ultimate failure has a direct effect on CFRP laminate notched strength [5, 6, 8, 10]. Intralaminar damage at the notch tip provides stress relief as the notch geometry changes and the stress concentration is reduced, hence increasing the notched strength. Larger damage zones typically provide more stress relief and hence greater notched strength. Conversely interlaminar damage, if extensive, reduces the notched strength as individual uncoupled plies are free to fail by the fracture mode of least resistance [9]. Damage initiation and progression is dependent on a number of variables such as stacking sequence, notch geometry, loading rate, test temperature etc. Concerning laminate lay-up and stacking sequence, Eriksson & Aronsson [6] showed 0º ply dominated laminates had higher notched strengths and exhibited more damage prior to failure than ±45º and 90º ply dominated laminates. Harris and Morris [9] carried out an in-depth study of the effect of laminate lay-up and stacking sequence and showed that laminate notched strength varied considerably with both the specified set of ply fibre orientations (i.e. lay-up), as well as the order in which the specific plies were arranged in the laminate (i.e. stacking sequence). Axial splits in the main load-carrying 0º plies were found to be particularly effective at reducing the notch stress concentration. Kortschot & Beaumont [10] showed that cross-ply laminates with blocked stacking sequences ($[90_2/0_2]_s$) exhibited more damage prior to failure and had 50% higher notched strength than laminates with a sub-laminate stacking sequence ($[90/0]_{2s}$), even though both had an equal number of 0º and 90º plies. Similarly, Green *et al.* [17] studied scaling effects for quasi-isotropic stacking sequences and found that sub-laminate scaled S_{OHT} decreased with increasing specimen size, but conversely, S_{OHT} increased with increasing specimen size for blocked stacking sequences. Harris and Morris [8] examined the effects of laminate thickness and found that in thick laminates, pre-failure damage near the notch only occurred in the outer plies; thus the greater the laminate thickness, the less effect damage had on the stress distribution prior to failure. Depending on the type of damage the laminate lay-up was susceptible to, the notched strength

either increased or decreased with thickness until a constant value for notched strength was achieved for laminates of 60 plies or more.

It has been shown by a number of researchers [4, 5, 10, 16] that CFRP laminate notched strength decreases with increasing notch size. One possible explanation for this was proposed by Whitney & Nuismer [18] for open hole laminates who showed that even though the stress concentration factor, K_T, is approximately 3 for holes of all sizes in quasi-isotropic OHT specimens, the stress drops off more steeply moving away from the hole, for smaller holes. It was reasoned that this increased the probability of having a large flaw in the highly stressed region around a large hole, resulting in a lower average strength for a laminate with a large hole.

A variety of through-thickness discontinuities have been used to determine the notched characteristics of CFRP laminates, *viz.* centre-cracked [4, 7], double edged notched [10] and open hole laminates [6, 16]. However, the open hole laminate has been adopted as the industry standard for determining the notched strength of FRP laminates [19 - 21]. Data presented in the literature for centre cracked and open hole tension laminates with the same lay-up and notch length indicates that the notched strength for both specimen types is not significantly different [6, 22].

The specific failure characteristics of individual FRPs are dependent on their constitutive material properties. Pinnell [13] showed that fibres with high tensile strength and modulus give greater strength as they provide better resistance to fibre-dominated tensile failure and enhance the ability to dissipate the stress concentration at the notch edge. In addition, a thermoplastic matrix system provided greater notched strength than a thermoset matrix system due to its greater strength and toughness [13]. Dimant *et al.* [23] compared the damage characteristics of notched, cross-ply Kevlar® fibre-reinforced plastic (KFRP) and E-glass fibre-reinforced plastic (GFRP). It was shown that the KFRP specimens exhibited similar damage initiation and growth behaviour as CFRP. Damage patterns were consistent and well-defined, involving transverse matrix cracks in the 90º plies and axial splits at the hole in the 0º plies, though the delaminations accompanying the axial splits form with a narrower tip angle than in CFRP. A greater density of transverse ply cracks and a greater tendency to delaminate was observed with increasing transverse ply thickness in GFRP. Fibre failure in the 0º ply occurred in the same plane coinciding with the transverse ply crack that

extended from the notch tip. The higher statistical variation in E-glass fibre strength lead to a more variable failure pattern in GFRP with multiple axial splits which spread far from the notch.

In recent years, high strength S2-glass fibre-reinforced composite materials have found increasing application in armour systems [24] and as a constituent material in the fibre metal laminate (FML) GLARE®, which is used in the upper fuselage of the Airbus A380 as well as other aerospace structural applications [24]. However, little data appears to be available in the literature on the damage characteristics of notched S2-Glass/epoxy composites.

The objective of this paper is to characterise and compare damage initiation and growth in open-hole tension CFRP and high strength S2-Glass FRP laminates. An experimental test series was carried out to determine laminate unnotched and open hole ultimate strength and strain of a CFRP and S2-glass FRP currently used in the aerospace industry. In addition, non-destructive inspection techniques were used to map damage growth with increasing applied load for both material systems. Four different stacking sequences were examined and in explaining the results, reference is made to basic material property tests which were also carried out on both systems.

2. Experimental Methods

The specimen geometry for the OHT specimens is shown in Fig. 1. All OHT specimens tested had a $2a/W$ ratio of 1/6, where $2a$ is the notch length (hole diameter) and W is the laminate width. The test procedure and specimen geometry were based on ASTM Standard D5766 [20]. Two FRP material systems were studied *viz.* Hexcel Materials Ltd. 6376C-HTA(12K)-5.5-29.5% CFRP and Cytec Engineered Materials Ltd. FM94-27%-S2-187-460 S2-glass GFRP. Four laminate stacking sequences were examined, one quasi-isotropic ($[45/0/-45/90]_{2s}$) and three cross-ply ($[90/0]_{4s}$, $[90/0]_{2s}$, $[90_2/0_2]_s$). These stacking sequences were chosen as quasi-isotropic type stacking sequences are very common in aircraft structures, while cross-ply stacking sequences of GFRP are used in GLARE® [25]. In addition, the $[90/0]_{2s}$ and $[90_2/0_2]_s$ stacking sequences were studied to examine the effects of sub-laminate and blocked stacking of plies in OHT laminates.

All test specimens were manufactured at the University of Limerick. Panels of the desired lay-up were prepared from prepreg and cured in an autoclave according to ASTM D5687 [28]. Test specimens were cut from the panels using a dedicated composite cutting machine with a diamond-coated cutting blade. In order to examine the initiation and growth of damage around the hole in the specimen, high quality holes free from defects associated with solid-tool drilling of composite materials, e.g. chip-out, surface delamination, internal delamination and fibre/matrix pull-out were generated using jigs and drilling methods developed as part of a previous study [27]. Laminates were sandwiched between two Perspex plates, to prevent chip-out on entry and exit, in a specialised jig. Holes were drilled and then reamed to their final dimensions using carbide tools, producing high quality holes for research purposes.

Five specimens of each laminate stacking sequence for both material systems were tested to failure to determine the average OHT strength (S_{OHT}). Three unnotched specimens, with the same dimensions as the OHT specimens, were also tested to failure to determine the average unnotched strength (S_{UN}) of each laminate. Each OHT specimen tested to failure was instrumented with two axial extensometers as shown in Fig. 2 to measure the localised displacement in the vicinity of the hole; extensometers remained attached right through to laminate final failure. Each extensometer had a gauge length of 25 mm and was placed on the specimen so that the hole was in the centre of the gauge length. Unnotched specimens were instrumented with one extensometer (that was removed prior to ultimate failure to prevent it being damaged) to determine displacements for comparison with OHT data. The use of hydraulically pressurised grips with specially machined faces for gripping composite materials ensured that all unnotched laminates failed in the gauge length. All specimens were loaded quasi-statically in tension, in stroke control at a rate of 0.03 mm/s (approximately 2 mm/min).

Having determined the S_{OHT} for each laminate, tests to percentages of S_{OHT} were carried out to map the initiation and progression of damage for each stacking sequence of both material systems. These OHT specimens were not instrumented with extensometers. Three percentage of S_{OHT} tests were carried out for quasi-isotropic laminates one each for 75%, 85% and 95% of S_{OHT}. Similarly, three percentage of failure tests were carried out for the $[90/0]_{4s}$ laminate (65%, 80% and 95% S_{OHT}), and four percentage of failure tests each for the $[90/0]_{2s}$

and $[90_2/0_2]_s$ (65%, 75%, 85% and 95% S_{OHT}). Damage progression in the vicinity of the hole in the CFRP specimens was examined using penetrant radiography; the penetrant used was iodomethane 99%. As damage voids (i.e. cracks and delamination) tend to close upon laminate unloading, the penetrant had to be applied to the laminate while it was subjected to a tensile load (usually 75% of the load it was previously subjected to; this allowed reopening of existing damage voids without causing new damage to form). A novel approach was developed to infuse penetrant into damage voids in the test specimens. A reservoir was created at the hole using two notched rubber blocks, stiffened with a steel backing plate, shown in Fig. 3a, and held in place using a G-clamp, as shown in Fig. 3b. The rubber blocks were carefully tightened onto the specimen to provide a liquid-tight seal around the hole, but not too tight to prevent re-opening of damage voids. Penetrant was added to the reservoir with a dropper and the specimen was held at the designated load for approximately 5 minutes. The penetrant level in the reservoir had to be repeatedly topped up during this time as firstly, the level drops as the penetrant infuses into the damage voids and secondly, Iodomethane 99% evaporates slowly at room temperature. Once sufficient time had elapsed for the penetrant to infuse into the damage voids, the laminate was unloaded and x-rayed. The quality of the radiograph was dependent on how quickly it was x-rayed after being removed from the straining frame, since the penetrant tended to evaporate out of the voids relatively quickly (10 – 15 minutes) after infusion. The above procedure was developed using considerable trial and error.

Both constituents of GFRP are translucent and so damage progression in specimens was examined using a backlight technique. Placing a bright light source behind the laminate reveals damage in the form of shadows. This method was found to produce damage progression images of a quality similar to that achieved by penetrant radiography and it was possible to examine (and video) the damage growth in real time.

In addition to the above tests, basic material tests were performed on 0º, 90º and ±45º specimens according to the appropriate standards [28, 29] to provide reference properties for both material systems. Further details on these tests can be found in [30].

3. Results and Discussion

3.1 Stress-strain curves and failure properties

Figure 4 shows the stress-strain curves for CFRP and GFRP unnotched and OHT specimens for each of the stacking sequences. Note that the unnotched curves are not to failure since the extensometers had to be removed prior to rupture to avoid damaging them. It is clear from these curves that the CFRP OHT specimens have greater strength and significantly greater stiffness than the GFRP OHT specimens; though not shown on these graphs, the same was also true for the unnotched specimens. However, the GFRP specimens (both unnotched and OHT) have a significantly greater ultimate strain and absorb greater strain energy (i.e. area under the stress-strain curve). These general property trends can be attributed to the fibre direction properties of each material. From the basic material property tests, it was found that CFRP is slightly stronger and has significantly greater stiffness in the fibre direction than GFRP, but has a significantly lower ultimate strain, as shown in Table 1.

Examination of unnotched and OHT stress-strain curves suggests that the presence of the hole has no effect on the stiffness of the CFRP laminates and only slightly reduces the stiffness of the GFRP laminates. This phenomenon can be attributed to the placement of the extensometers on the specimen (see Fig. 2). When load is applied, the unnotched specimen displacement within the extensometer gauge length is uniform across the laminate width. However, for the OHT specimen, greater strain occurs along the centre away from the edges due to the stress concentration at the hole, and as the load increases, due to damage initiation and propagation in the region around the hole. This is not detected by the extensometers as their attachment points are relatively remote from the high strain region. Therefore, the stress-strain ratio appears similar for OHT and unnotched specimens.

Strength data is presented in Table 2 showing good repeatability for each data series, with a maximum coefficient of variance of 5%. The unnotched strength is seen to be significantly greater than the OHT strength for all laminate stacking sequences of both material systems. Normalised strength (S_{OHT}/S_{UN}) data is presented for each laminate. The normalised strength is a measure of the notch sensitivity of each of the laminate lay-ups. According to [14], a material is ideally notch insensitive (ideally ductile) if the failure stress is proportional to the net-sectional area, whereas it is ideally notch sensitive (brittle) if it fails when the local stress at the edge of the hole equals the unnotched strength (S_{UN}). In general, an open hole specimen with a $2a/W$ ratio of 1/6 has a notch insensitive normalised strength ($1-2a/W$) of 5/6 (≈ 83%) [14]. Conversely, an open hole specimen (again with $2a/W = 1/6$) has a

notch sensitive normalised strength = $1/K_T$ [14], where K_T is the stress concentration factor. For a quasi-isotropic lay-up, K_T is approximately 3, yielding a notch sensitive normalised strength of 0.32 [14], while a cross-ply lay-up yields 0.22 for GFRP and 0.19 for CFRP (K_T for each laminate was determined analytically according to the equations given in [22] with finite-width correction factors determined from [31]). This type of analysis gives the range of notch sensitive – notch insensitive bands using in the following analysis.

For the current study, the $[90_2/0_2]_S$ laminate achieves the highest normalised strength (S_{OHT}/S_{UN}), 0.85 for CFRP and 0.59 for GFRP. Based on the above analysis, the high normalised strength achieved by the CFRP $[90_2/0_2]_S$ laminate indicates that it is notch insensitive. This is supported by the radiograph shown in Fig. 9h, which shows long axial splits in the 0º plies on each side of the hole at 95% S_{OHT}, indicating that the load is only being supported by the two outer unnotched ligaments of the laminate, the stress concentration at the hole is completely blunted. All the other laminates fall well within the notch sensitive – notch insensitive bands. The CFRP and GFRP quasi-isotropic laminates have approximately the same normalised strength, 0.53 and 0.54 respectively. However, the CFRP cross-ply laminates attain higher normalised strengths than the GFRP laminates, suggesting that overall, CFRP is less notch sensitive.

Comparison of the strength data for $[90/0]_{4s}$ and $[90/0]_{2s}$ in Table 2 shows the effect which laminate thickness has on notched strength. Both laminates have the same stacking sequence, but $[90/0]_{4s}$ is twice as thick. The S_{UN} values for $[90/0]_{4s}$ and $[90/0]_{2s}$ are not significantly different for both material systems. However, the S_{OHT} of the $[90/0]_{2s}$ laminate is significantly higher than that of the $[90/0]_{4s}$ laminate for both material systems.

Comparison of the data for $[90/0]_{2s}$ and $[90_2/0_2]_S$ shows the effect which stacking sequence has on notched strength. Both laminates have the same thickness and contain equal numbers of 0º and 90º plies, but the $[90/0]_{2s}$ laminate has a sub-laminate stacking sequence, while the $[90_2/0_2]_S$ laminate has a blocked-ply stacking sequence. The S_{UN} of the $[90/0]_{2s}$ and $[90_2/0_2]$s laminates are not significantly different for both material systems. However, the $[90_2/0_2]_s$ laminate S_{OHT} is significantly higher than the $[90/0]_{2s}$ laminate S_{OHT} for both CFRP (56 %) and GFRP (35 %). This finding is similar to observations made by Kortschot and Beaumont [10] for CFRP double-edged notched specimens with the same stacking sequences.

A comparison of OHT laminate stress-strain and modulus reduction curves for all lay-ups is presented in Fig. 5. The modulus reduction curves were generated by calculating the slope of the stress-strain curves using a moving average window size of 7. For CFRP, the quasi-isotropic OHT laminate has the lowest modulus (approximately 47 GPa), the $[90/0]_{2s}$ and $[90_2/0_2]_s$ laminates achieve a higher modulus of about 65 GPa, and the $[90/0]_{4s}$ laminate achieves the highest modulus of approximately 70 GPa. A similar trend is observed for the GFRP OHT laminates. The quasi-isotropic laminate has the lowest modulus (approximately 17 GPa), while all the cross-ply laminates achieve a slightly higher modulus of about 23.5 GPa. This data indicates that notched laminate stiffness depends on the stiffness of the reinforcing fibres as well as the percentage of fibres aligned in the direction of loading, i.e. the stiffer laminates have a greater percentage of plies aligned with the direction of loading, as expected.

Examination of the modulus reduction curves in Fig. 5 shows that for GFRP a reduction in modulus between 0% and 0.5% strain occurs in all cases. This is not seen in the CFRP curves. This reduction in modulus is attributed to yielding of the matrix in the 90º plies. GFRP exhibits significant non-linear transverse behaviour and modulus reduction as demonstrated by experimental curves obtained from 90º specimen tensile tests shown in Fig. 6. The 90º specimen exhibits a steady reduction in modulus between 0% and 0.5% strain, after which the modulus starts to plateau, similarly to the behaviour exhibited by the GFRP OHT specimens. In contrast CFRP 90º specimens show that no such non-linear behaviour (see Fig. 6) and consequently no such modulus reduction in the OHT configuration (apart from slight variations due to bedding in of the specimens in the grips).

3.2 Damage Progression Mapping

The progression of damage in CFRP and GFRP quasi-isotropic OHT specimens is shown in Fig. 7. Damage does not occur until a relatively high load is reached (i.e. approximately 75% of S_{OHT}). Radiographs of the CFRP specimen at 75% and 85% S_{OHT} shows that damage mostly consists of matrix cracking in the ±45° and 90° plies in the vicinity of the hole, accompanied by some delamination around the hole; cracks in the 90° plies extend to the laminate edge at 85% S_{OHT}. However, between 85% and 95% S_{OHT} large triangular delamination zones emanate from the hole, decoupling plies and leading to rapid

failure of the laminate (Note: areas of delamination shown around the hole at 75% and 85% S_{OHT} in Figs. 7a and 7c, are not visible at 95% S_{OHT} in Fig. 7e due to evaporation of the penetrant). Backlight images of the GFRP laminate show a quite similar trend for damage propagation. At 85% and 90% of S_{OHT} shadows in the vicinity of the hole indicated the presence of matrix cracks in the ±45° and 90° plies; the shadows are quite faint however and matrix cracking does not appear to be as extensive as in CFRP at this point in the loading cycle. At 95% of S_{OHT} however, deep shadows around the hole indicate the formation of delamination zones just prior to failure, in a similar manner to that of CFRP.

Damage progression in CFRP and GFRP $[90/0]_{4s}$ laminates is presented in Fig. 8. Damage in the $[90/0]_{4s}$ laminate is characterised by axial splits at each side on the hole in the 0° plies. Radiographs of the CFRP laminate indicate that axial splits occur in the 0° plies prior to 65% S_{OHT} and are accompanied by matrix cracks in the 90° plies. As the load increases, the damage zone increases in size, but the matrix cracks in the 90° plies only occur outside (i.e. towards the laminate edge) of the 0° ply axial splits indicating that the splits effectively blunt the stress concentration from the hole. Backlight images of the GFRP $[90/0]_{4s}$ OHT laminate indicate a similar well defined pattern of two axial splits in the 0° plies (shown as linear shadows either side on the hole) which increase in length with increasing load. The splits are longer than those observed in the CFRP laminates but evidence of matrix cracking in the 90° plies is again faint in comparison to CFRP. The apparently lower level of matrix cracks in the 90° plies in the GFRP OHT specimens compared to the CFRP OHT specimens may be due to the less brittle nature of the matrix material in GFRP, as evidenced in Fig. 6. The well-defined, consistent pattern of damage in the GFRP specimens is in contrast to the findings of Dimant et al. [23] for E-glass FRP, which showed a variable pattern of multiple axial splits across the width of the specimens; the variability in behaviour was attributed in [23] to the relatively high statistical variance in the strength of E-glass fibres. The present results demonstrate that high-strength S2-glass FRP is closer to a high-performance CFRP material in its notched failure behaviour, than it is to E-glass FRP.

Radiographs of damage progression in CFRP $[90/0]_{2s}$ and $[90_2/0_2]_s$ OHT laminates, presented in Fig. 9, show that damage is again characterised by axial splits in the 0° plies accompanied by matrix cracks in the 90° plies. However, the damage zones in the $[90_2/0_2]_s$ OHT laminate are much more extensive than those in the $[90/0]_{2s}$ laminate (or indeed the

$[90/0]_{4s}$ laminate in Fig. 8). The length of the axial splits observed in the $[90_2/0_2]_s$ laminate radiographs indicates that blocked stacking of 0° plies facilitates the growth of this form of damage, whereas placing 90° plies between each 0° ply, as in the sub-laminate stacked $[90/0]_{2s}$ laminate, tends to arrest the growth of the splits more. This result is consistent with the findings of [10]. In addition, areas of triangular delamination are evident along the length of the axial splits in both stacking sequences, particularly from 75% S_{OHT} to failure. The edge of the delamination zone in the $[90_2/0_2]_s$ radiographs appears as a 'tide-mark', due to evaporation of penetrant prior to x-ray exposure. Again, the extensive matrix cracking in the 90° plies occurs mainly outside of the axial splits showing the effective stress concentration blunting of this form of damage.

Backlight images of damage progression in GFRP $[90/0]_{2s}$ and $[90_2/0_2]_s$ OHT laminates presented in Fig. 10 show a similar trend to that exhibited by CFRP. However, as with the $[90/0]_{4s}$ GFRP laminates evidence of 90° ply matrix cracking, while clearer than in the $[90/0]_{4s}$ case, is quite faint in comparison to the CFRP specimens.

Comparison of the damage in the $[90/0]_{4s}$ (Fig. 9) and $[90/0]_{2s}$ (CFRP in Fig. 9 and GFRP in Fig.10) OHT laminates shows that although both have the same stacking sequence and exhibit similar damage patterns, the damage zones, and particularly the length of the axial splits, are significantly greater in the $[90/0]_{2s}$ OHT laminate, for both material systems. This can be attributed to the formation of triangular zones of delamination along the length of the axial splits, particularly evident at 85% and 95% S_{OHT}, which facilitate their increasing growth as they are freed from transverse reinforcing provided by the 90° ply fibres. The thin $[90/0]_{2s}$ laminate (8 plies) is more susceptible to delamination than the thicker $[90/0]_{4s}$ laminate (16 plies) as interlaminar stresses tend to be higher in the surface plies of laminates, hence a greater percentage of the plies in the $[90/0]_{2s}$ laminate are subjected to these higher interlaminar stresses than in the $[90/0]_{4s}$ laminate.

Comparison of the damage progression maps for the cross-ply laminates ($[90/0]_{4s}$, $[90/0]_{2s}$ and $[90_2/0_2]$s) with strength data (Table 2) shows that there is a correlation between the extent of damage sustained by a laminate prior to failure and the S_{OHT}. The $[90_2/0_2]_S$ laminate achieves the highest S_{OHT} value and also exhibits the greatest amount of damage prior to failure, for both material systems. Conversely, the $[90/0]_{4s}$ laminate has the lowest S_{OHT} of the cross-ply laminates while exhibiting the least damage prior to failure. In addition,

stress-strain curves (Fig. 5) indicate that laminates that sustain significant damage prior to failure absorb greater energy before failure. The principal at work here is that damage formation, effectively blunts the stress concentration due to the notch, allowing the specimen to achieve higher S_{OHT} values and energy absorbed to failure. These findings are consistent with those in [8, 9, 10].

Comparing the quasi-isotropic and $[90/0]_{4s}$ configurations, which both have the same thickness, a similar principle can be seen to be at work. Even though the $[90/0]_{4s}$ laminate has a much higher unnotched strength than the quasi-isotropic laminate (1112 MPa versus 705 MPa for CFRP and 937 MPa versus 654 MPa for GFRP), the normalised strength (S_{OHT}/S_{UN}) is significantly higher for the quasi-isotropic configuration for both material systems indicating lower notch sensitivity. Comparing Figs. 7 and 8, it can be seen that more extensive damage occurs prior to failure in the quasi-isotropic configuration.

4. Concluding Remarks

Comparing the two materials tested in this study, the CFRP OHT specimens had the greater stiffness and strength, while the GFRP OHT specimens exhibited greater strain to failure and significantly higher toughness. Comparison of damage progression in the two materials however indicates a very similar damage and failure sequence. In the quasi-isotropic configuration, this consisted of matrix cracks in the ±45º and 90º plies followed by extensive delamination prior to failure. In the cross-ply configuration, it consisted of matrix cracks in the 90º plies, a pair of axial splits emanating from each side of the hole in the 0º plies and triangular areas of delamination extending from the splits. This regular and consistent pattern of damage formation in the current S2-glass composite is in contrast to the more variable damage patterns involving multiple axial splits exhibited by E-glass composite in [23].

A correlation was found for all lay-ups between the extent of damage prior to failure and the resulting S_{OHT} and energy absorbed. Higher levels of damage formation (provided plies are still coupled to each other) reduce the stress concentration and result in higher S_{OHT} values and energy absorbed to failure. The large difference in S_{OHT} between blocked and sub-laminate level stacking sequences in the cross-ply laminates is an illustration of this point, with blocked sequences allowing easier growth of the splits in the 0º plies, resulting in more extensive damage in the specimen and greatly increased energy absorbed. Thicker cross-ply

laminates with the same stacking sequence were also found to have shorter axial splits and consequently lower S_{OHT} and energy absorbed.

The transverse behaviour of GFRP is highly non-linear as exhibited by tests on 90º specimens. In the OHT tests this shows up in the form of a drop in stiffness early in the test (between 0 and 0.5% strain), and a reduced level of matrix cracking in the 90º plies (compared to CFRP). This reduced level of matrix cracking in the 90º plies may have knock on effects in cross-ply OHT configurations in that it provides more resistance to growth of splits in the adjacent 0º plies than the highly cracked 90º plies in the CFRP specimens. As seen above, limiting the growth of axial splits results in lower S_{OHT} values and this may be the reason why GFRP was found here to be more notch sensitive (i.e. having lower S_{OHT}/S_{UN} values) than CFRP.

Acknowledgements

This work was funded by the Irish Research Council for Science, Engineering and Technology (IRCSET) Basic Research Project Grant: A Study of Damage Initiation and Growth in Composite Bolted Joints; Project No. SC/02/191. One author (R.M. O'Higgins) would like to acknowledge the funding provided by the University of Limerick Foundation H.T. Hallowell scholarship. The authors would like to thank Mr. Declan Kenihan for his advice and help with the radiographs.

References

1. Flower HM, Soutis C. Materials for Airframes. The Aeronautical Journal 2003; 107 (1072): 331 – 341.

2. Awerbuch J, Madhukar MS. Notched Strength of Composite Laminates: Predictions and Experiments – A Review. Journal of Reinforced Plastics and Composites 1985; 4: 1 – 159.

3. Backland J, Aronsson CG. Tensile Fracture of Laminates with Holes. Journal of Composite Materials 1986; 20: 259 – 286.

4. Coats TW, Harris CE. A Progressive Damage Methodology for Residual Strength Predictions of Notched Composite Panels. Journal of Composite Materials 1999; 33: 2193 – 2224.

5. de Morais AB. Open-Hole Strength of Quasi-Isotropic Laminates. Composites Science and Technology 2000; 60: 1997 – 2004.

6. Eriksson I, Aronsson CG. Strength of Tensile Loaded Graphite/Epoxy Laminates Containing Cracks, Open and Filled Holes. Journal of Composite Materials 1990; 24: 456 – 482.

7. Harris CE, Morris DH. On the Use of Crack-Tip-Opening Displacement to Predict the Fracture Strength of Notched Graphite/Epoxy Laminates. Experimental Mechanics 1985; 25 (2): 193 – 199.

8. Harris CE Morris DH. Fracture of Thick Laminated Composites. Experimental Mechanics 1986; March: 34 – 41.

9. Harris CE, Morris DH. A Fractographic Investigation of the Influence of Stacking Sequence on the Strength of Notched Laminated Composites. Fractography of Modern Engineering Materials: Composites and Metals ASTM STP 948; Masters JE, Au JJ, Eds.: American Society for Testing and Materials, Philadelphia. 1987; 131 – 153.

10. Kortschot MT, Beaumont PWR. Damage Mechanics of Composite Materials: - I – Measurements of Damage and Strength. Composites Science and Technology 1990; 39: 289 – 301.

11. Lee J, Soutis C. A Study on the Compressive Strength of Thick Carbon Fibre-Epoxy Laminates. Composites Science and Technology 2007; 67 (10): 2015-2026.

12. O'Higgins RM, Padhi GS, McCarthy MA, McCarthy CT. Experimental and numerical Study of the Open-Hole Tensile Strength of Carbon/Epoxy Composites. Mechanics of Composite Materials 2004; 40 (4), 269-278.

13. Pinnell MF. An Examination of the Effect of Composite Constituent Properties on the Notched Strength Performance of Composite Materials. Composites Science and Technology 1996; 56: 1405-1413.

14. Soutis C, Fleck NA. Static Compression Failure of Carbon Fibre T800/924C Composite Plate with a Single Hole. Journal of Composite Materials 1990; 24: 536–558.

15. Spearing SM, Beaumont PWR. Fatigue damage mechanics of composite materials I: Experimental measurement of damage and post-fatigue properties. Composites Science and Technology 1992; 44: 159 – 168.

16. Wang J, Callus PJ, Bannister MK. Experimental and Numerical Investigation of the Tension and Compression Strength of Un-notched and Notched Quasi-Isotropic Laminates. Composite Structures 2004; 64: 297 – 306.

17. Green BG, Wisnom MR, Hallet SR. An experimental investigation into the tensile strength scaling of notched composites. Composites: Part A 2007; 38: 867 – 878.

18. Whitney JM, Nuismer RJ. Stress Fracture Criteria for Laminated Composites Containing Stress Concentrations. Journal of Composite Materials 1974; 8: 253 – 265.

19. AITM (Airbus Industrie Test Method) 1-0007. Fibre Reinforced Plastics: Determination of Notched, Unnotched and Filled Hole Tensile Strength. June 2001.

20. ASTM Standard D5766/D5766M – 02. Standard Test Method for Open Hole Tensile Strength of Polymer Matrix Composite Laminates. Annual Book of ASTM Standards 2002; 15.03.

21. ASTM Standard D6484/D6484M – 99. Standard Test Method for Open-Hole Compressive Strength of Polymer Matrix Composite Laminates. Annual Book of ASTM Standards 1999; 15.03.

22. Daniel IM, Ishai O. Engineering Mechanics of Composite Materials. Oxford University Press, New York, 1994.

23. Dimant RA, Shercliff HR, Beaumont PWR. Evaluation of a Damage-Mechanics Approach to the Modelling of Notched Strength in KFRP and GRP Cross-Ply Laminates. Composites Science and Technology 2002; 62 (2): 255 – 263.

24. Hosur MV, Vaidya UK, Myers D, Jeelani S. Studies on the repair of ballistic impact damaged S2-glass/vinyl ester laminates. Composite Structures 2003; 61: 281 – 290.

25. Vlot A, Vogelesang LB, de Vries TJ. Towards Application of Fibre Metal Laminates in Large Aircraft. Aircraft Engineering and Aerospace Technology 1999; 71 (6): 558 – 570.

26. ASTM Standard D5687/D5687M – 95(2002). Guide for Preparation of Flat Composite Panels with Processing Guidelines for Specimen Preparation. Annual Book of ASTM Standards 2002; 15.03.

27. McCarthy MA, Lawlor VP, Stanley WF, McCarthy CT. Bolt-hole clearance effects and strength criteria in single-bolt, single-lap, composite bolted joints. Composites Science and Technology 2002; 62: 1415 – 1431.

28. ASTM Standard D3039/D3039M – 00. Standard Test Method for Tensile Properties of Polymer Matrix Composite Materials. Annual Book of ASTM Standards 2000; 15.03.

29. ASTM Standard D3518/D3518M – 94 (2001). Standard Test Method for In-Plane Shear Response of Polymer Matrix Composite Materials by Tensile Test of a ±45º Laminate. Annual Book of ASTM Standards 2001; 15.03.

30. O'Higgins RM. An Experimental and Numerical Study of Damage Initiation and Growth in High Strength Glass and Carbon Fibre-Reinforced Composite Materials. PhD Thesis, University of Limerick, Department of Mechanical and Aeronautical Engineering, 2007.

31. Tan SC. Finite-width correction factors for anisotropic plate containing a central hole. Journal of Composite Materials 1988; 22: 1080 – 1097.

Fig. 1. Open hole tension specimen geometry (all dimensions in mm)

Fig. 2. Open Hole Tension (OHT) specimen test set-up

Fig. 3. Penetrant application method.

Fig. 4. Comparison of unnotched (UN) and open hole tension (OHT) specimen stress-strain curves for all four stacking sequences and two materials. (* Unnotched stress-strain curves are not to failure due to extensometer removal prior to rupture)

Fig. 5. Comparison of OHT laminate stress-strain and modulus reduction curves for different stacking sequences

Fig. 6. CFRP and GFRP transverse material behaviour data

Fig. 7. Damage progression in CFRP and GFRP quasi-isotropic OHT laminates

Fig. 8. Damage progression in CFRP and GFRP $[90/0]_{4s}$ OHT laminates

Fig. 9. Comparison of damage progression in CFRP $[90/0]_{2s}$ and $[90_2/0_2]_s$ OHT laminates

Fig. 10. Comparison of damage progression in GFRP $[90/0]_{2s}$ and $[90_2/0_2]_s$ OHT laminates

Table 1 Material properties

Property	CFRP	GFRP
E_{11} (GPa)*	139	52
E_{22} (GPa)*	10	10
G_{12} (GPa) †	5.2	3.0
ν_{12}*	0.32	0.28
S_{11} (MPa)*	2170	1840
S_{22} (MPa)*	73	44
S_{12} (MPa) †	83	39
e_{11} (%)*	1.5	3.8
e_{22} (%)*	0.8	1.0

* calculated according to ASTM D3039 [28]
† calculated according to ASTM D3518 [29]

Table 2 **Unnotched (UN) and open hole tension (OHT) laminate strength data**

Lay-up	**$[45/0/-45/90]_{2s}$**			**$[90/0]_{4s}$**			**$[90/0]_{2s}$**			**$[90_2/0_2]_s$**		
CFRP Data												
	S_{UN} (MPa)	**S_{OHT} (MPa)**	**S_{OHT}/S_{UN} (%)**	**S_{UN} (MPa)**	**S_{OHT} (MPa)**	**S_{OHT}/S_{UN} (%)**	**S_{UN} (MPa)**	**S_{OHT} (MPa)**	**S_{OHT}/S_{UN} (%)**	**S_{UN} (MPa)**	**S_{OHT} (MPa)**	**S_{OHT}/S_{UN} (%)**
Average Value	710	380	53	1110	480	45	1060	550	52	1010	860	85
S.D. (C.V. {%})	17 (2.4)	7 (1.9)	-	16 (1.5)	12 (2.4)	-	54 (5.2)	28 (5.1)	-	39 (3.8)	22 (2.6)	-
GFRP Data												
	S_{UN} (MPa)	**S_{OHT} (MPa)**	**S_{OHT}/S_{UN} (%)**	**S_{UN} (MPa)**	**S_{OHT} (MPa)**	**S_{OHT}/S_{UN} (%)**	**S_{UN} (MPa)**	**S_{OHT} (MPa)**	**S_{OHT}/S_{UN} (%)**	**S_{UN} (MPa)**	**S_{OHT} (MPa)**	**S_{OHT}/S_{UN} (%)**
Average Value	660	350	54	940	370	40	900	410	46	960	560	59
S.D. (C.V. {%})	12 (1.8)	10 (2.9)	-	8 (1.0)	4 (1.0)	-	37 (4.1)	14 (3.4)	-	20 (2.1)	17 (3.0)	-

Figure 1

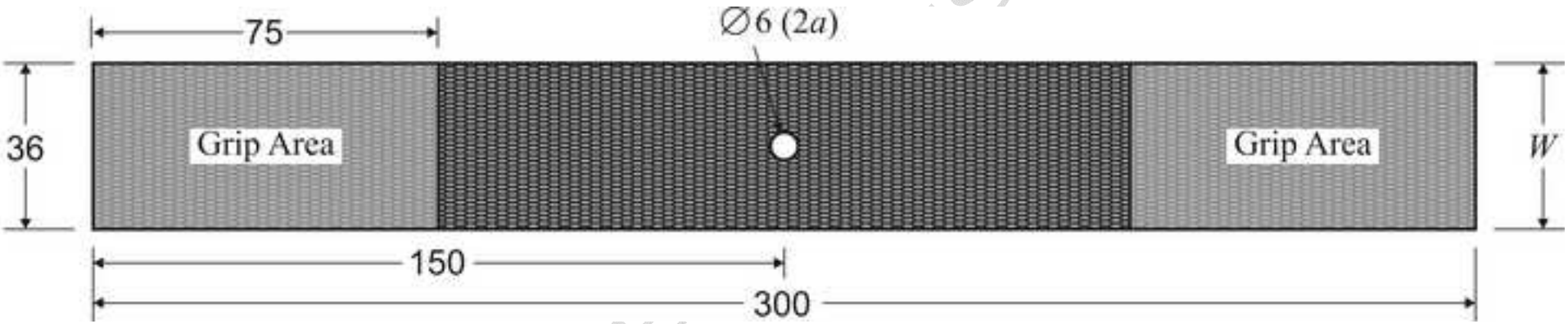

Figure 2

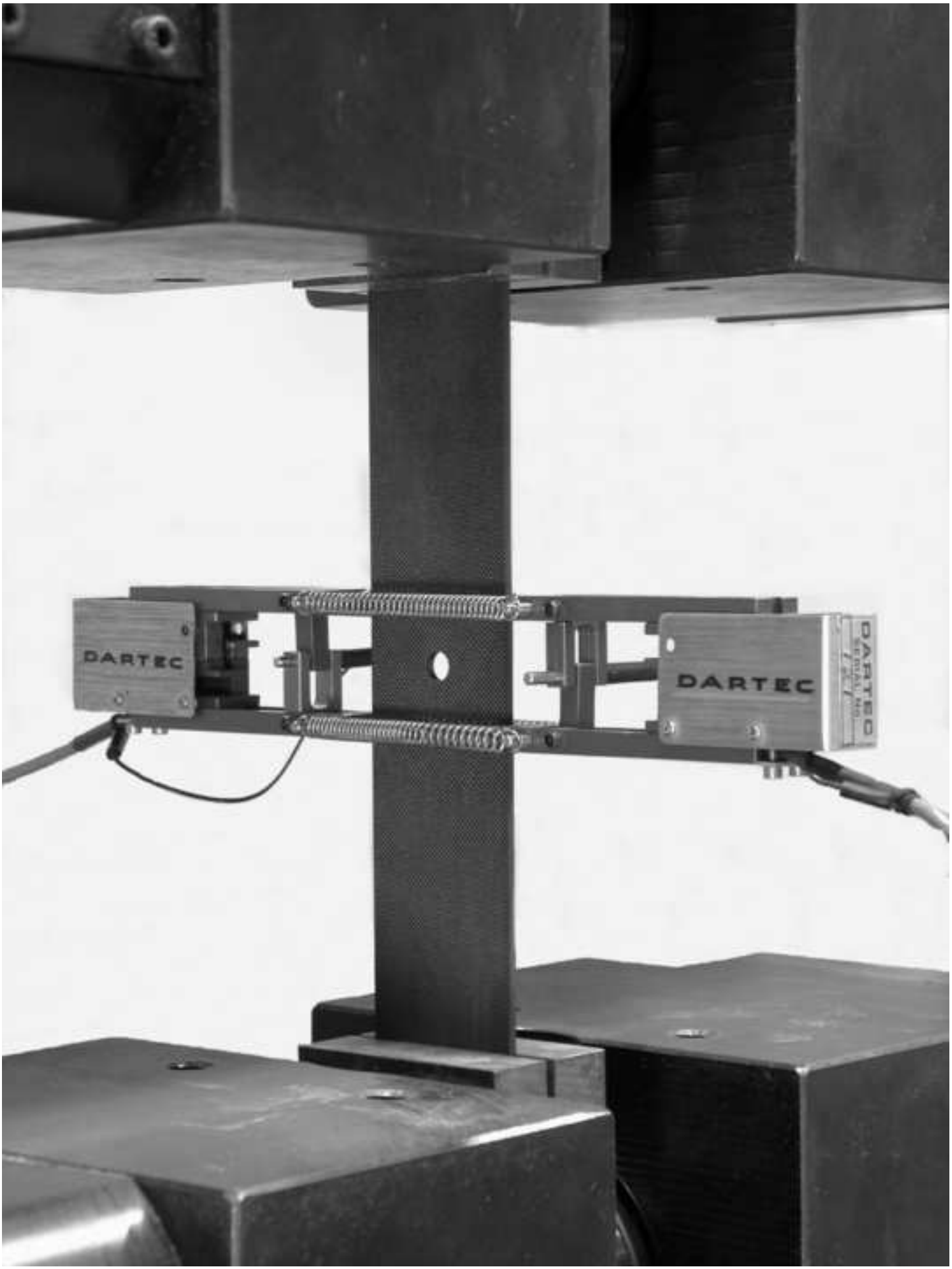

Figure 3

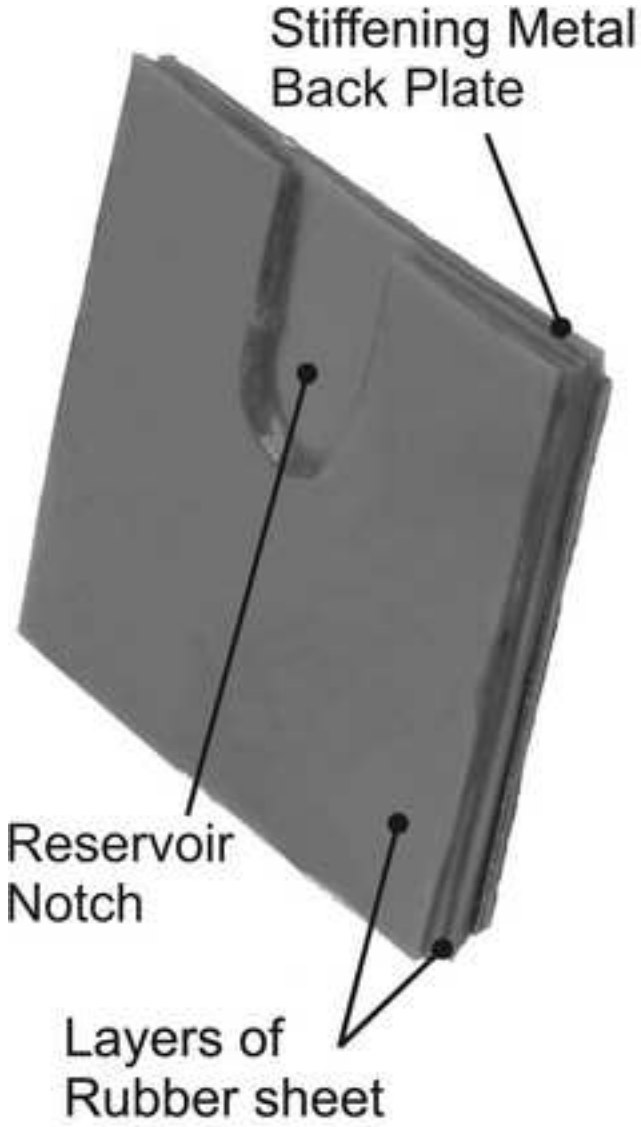

(a) Notched rubber reservoir block

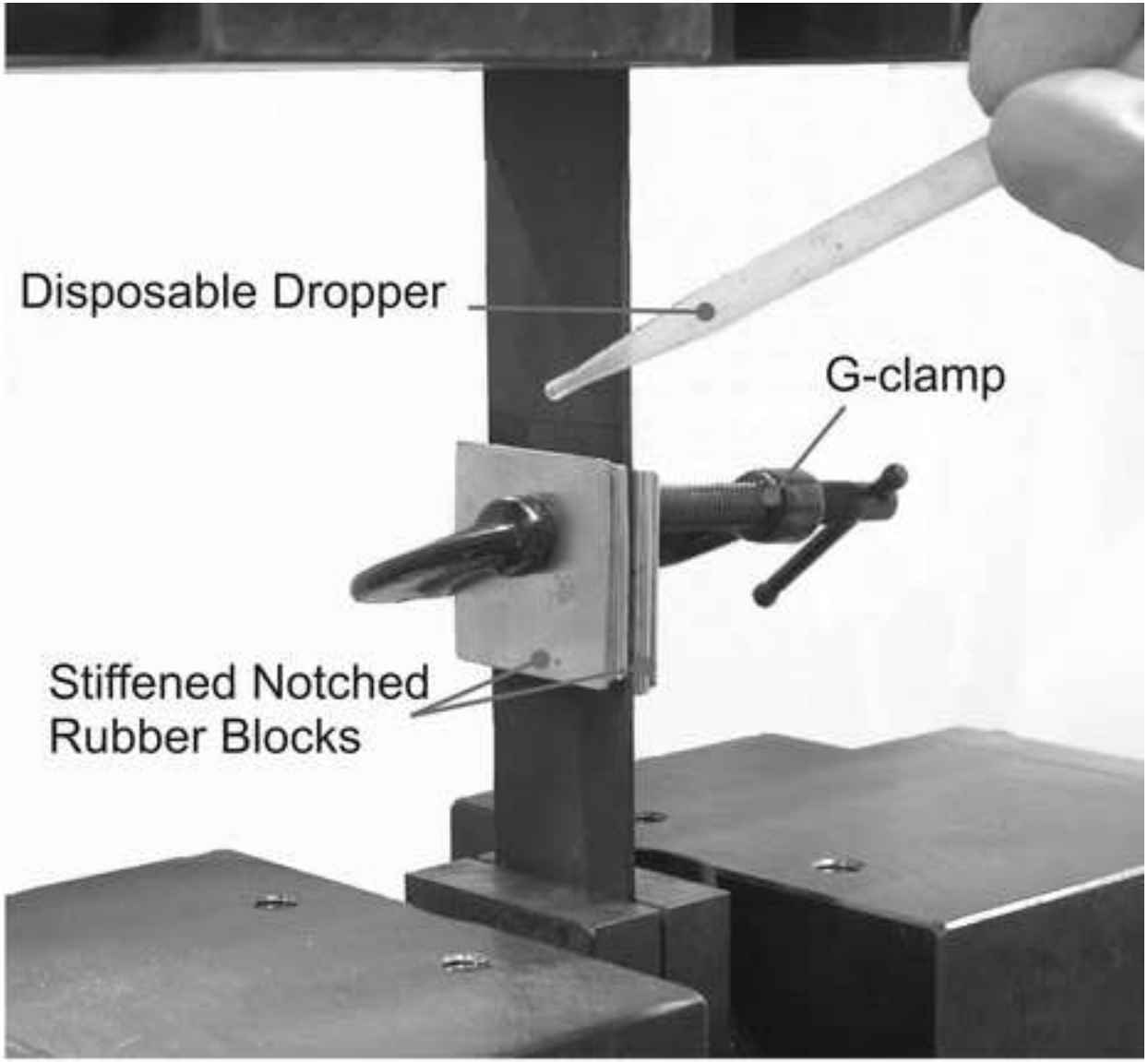

(b) Set-up for penetrant infusion

Figure 4

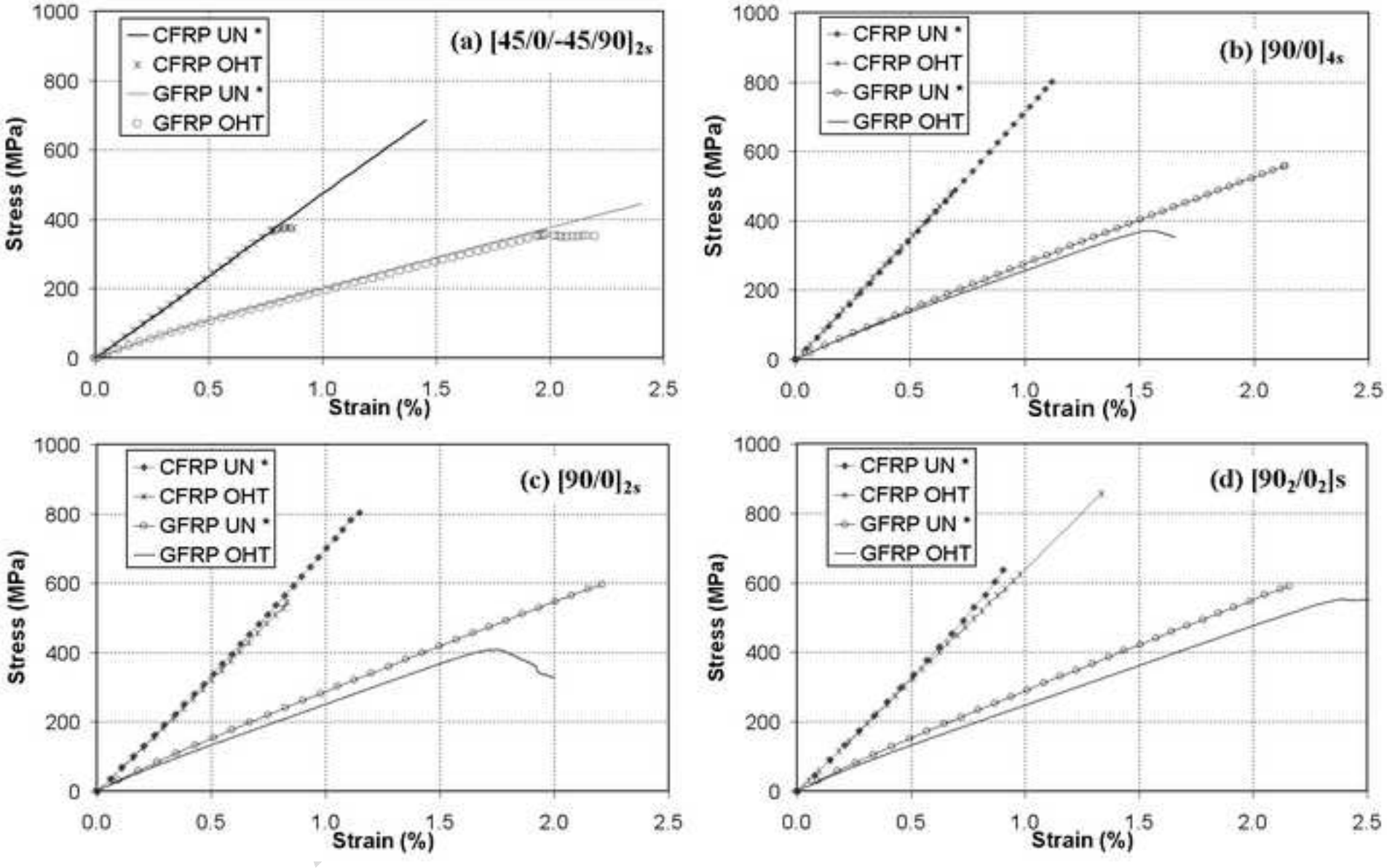
(a) [45/0/-45/90]2s
(b) [90/0]4s
(c) [90/0]2s
(d) [90₂/0₂]s
CFRP UN *
CFRP OHT
GFRP UN *
GFRP OHT
Stress (MPa)
Strain (%)
0
200
400
600
800
1000
0.0
0.5
1.0
1.5
2.0
2.5

Figure 5

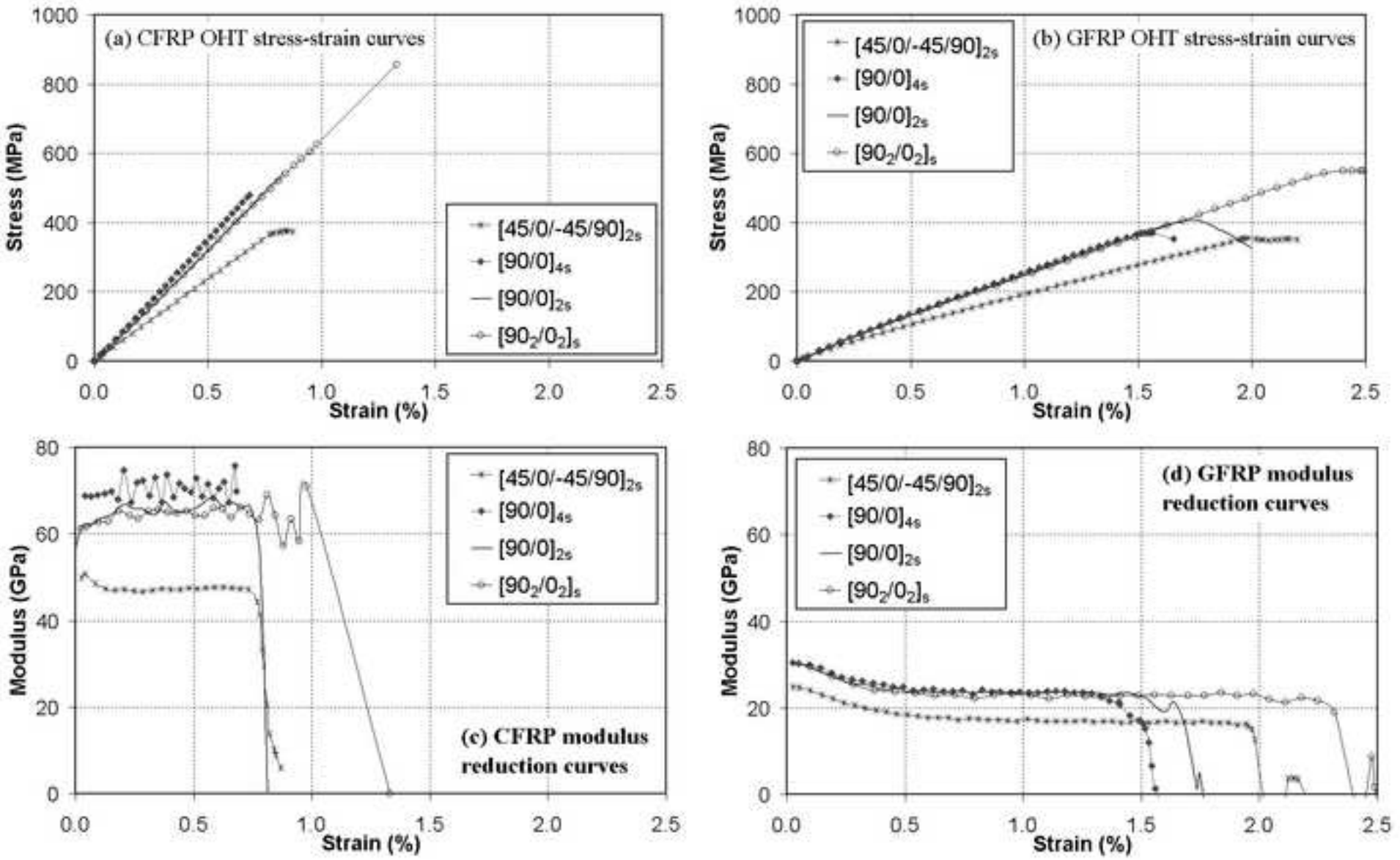
(a) CFRP OHT stress-strain curves
Stress (MPa)
Strain (%)
[45/0/-45/90]2s
[90/0]4s
[90/0]2s
[902/02]s
(b) GFRP OHT stress-strain curves
Stress (MPa)
Strain (%)
[45/0/-45/90]2s
[90/0]4s
[90/0]2s
[902/02]s
(c) CFRP modulus reduction curves
Modulus (GPa)
Strain (%)
[45/0/-45/90]2s
[90/0]4s
[90/0]2s
[902/02]s
(d) GFRP modulus reduction curves
Modulus (GPa)
Strain (%)
[45/0/-45/90]2s
[90/0]4s
[90/0]2s
[902/02]s

Figure 6

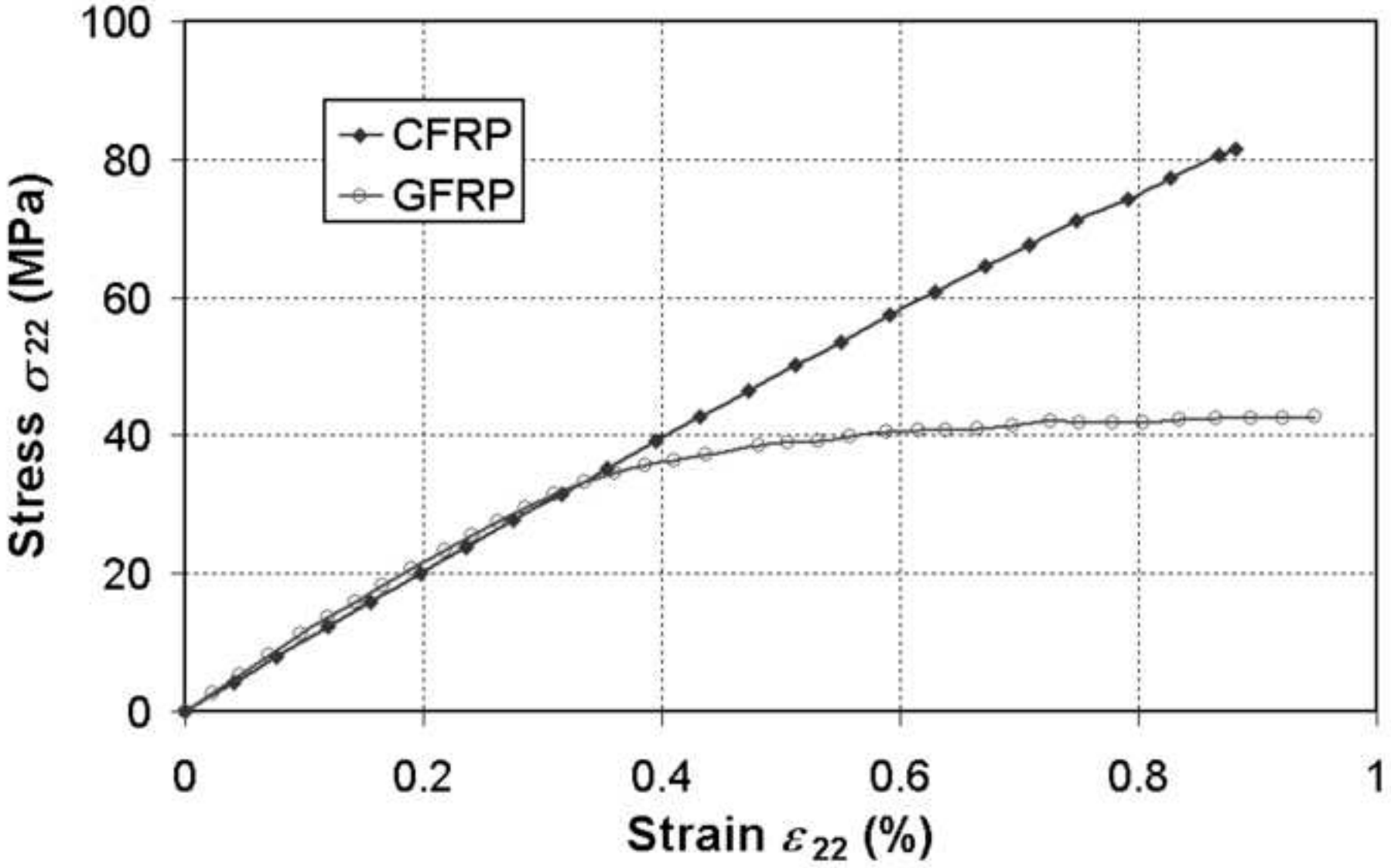
CFRP
GFRP
Stress σ_{22} (MPa)
Strain ε_{22} (%)
0
20
40
60
80
100
0
0.2
0.4
0.6
0.8
1

Figure 7

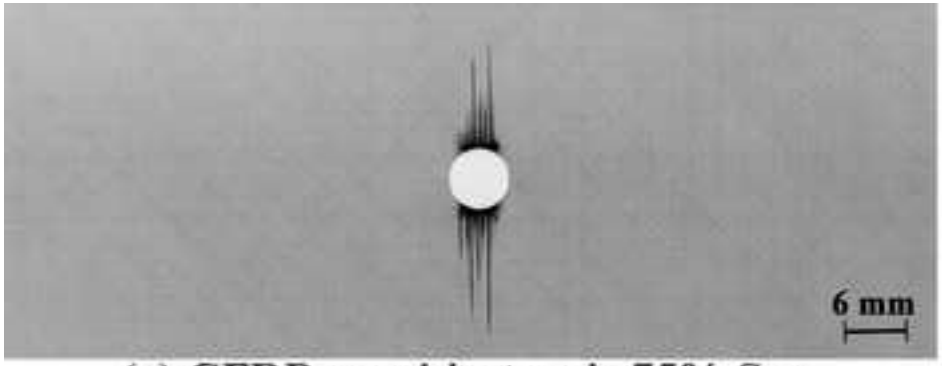

(a) CFRP quasi-isotropic 75% S_{OHT}

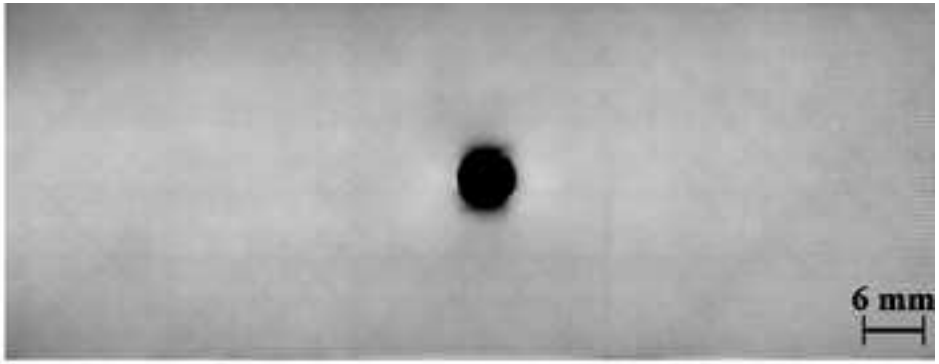

(b) GFRP quasi-isotropic 75% S_{OHT}

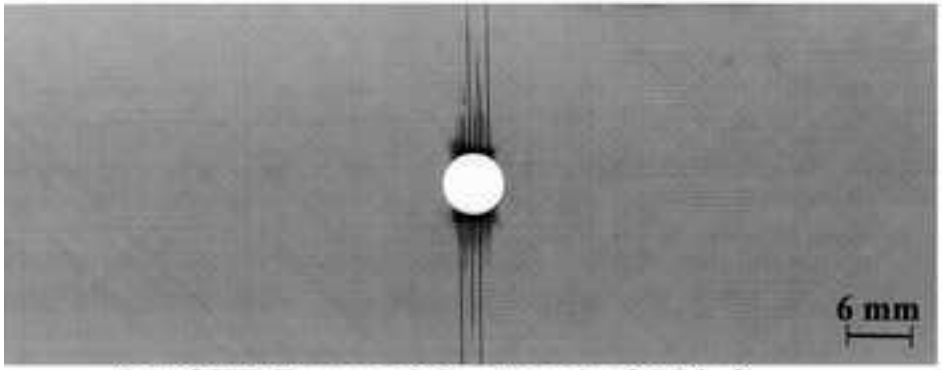

(c) CFRP quasi-isotropic 85% S_{OHT}

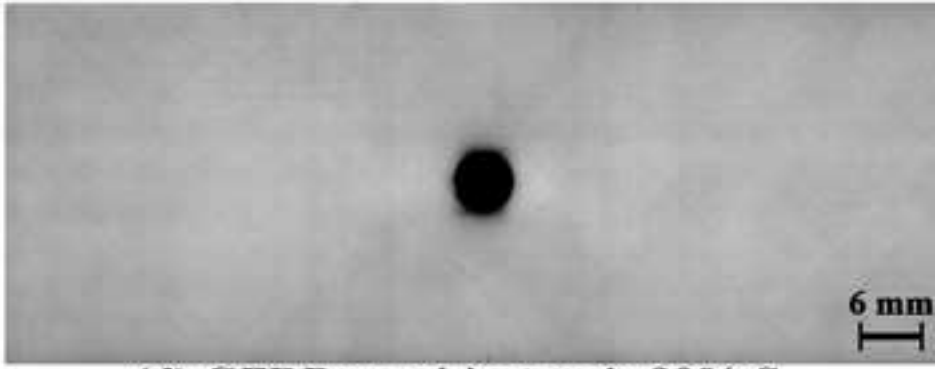

(d) GFRP quasi-isotropic 90% S_{OHT}

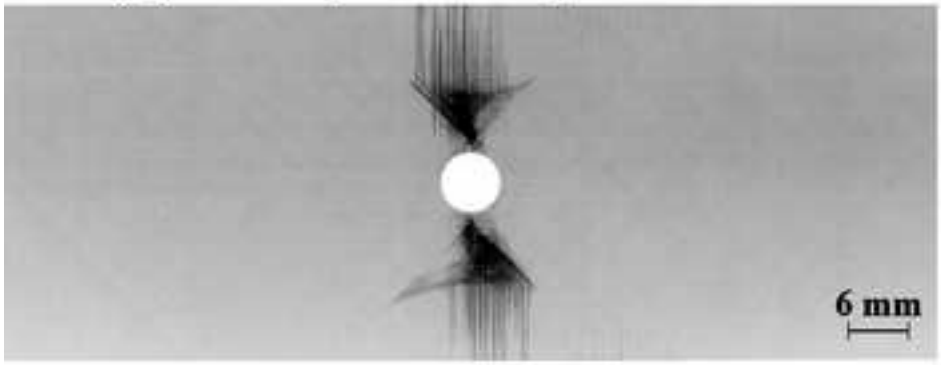

(e) CFRP quasi-isotropic 95% S_{OHT}

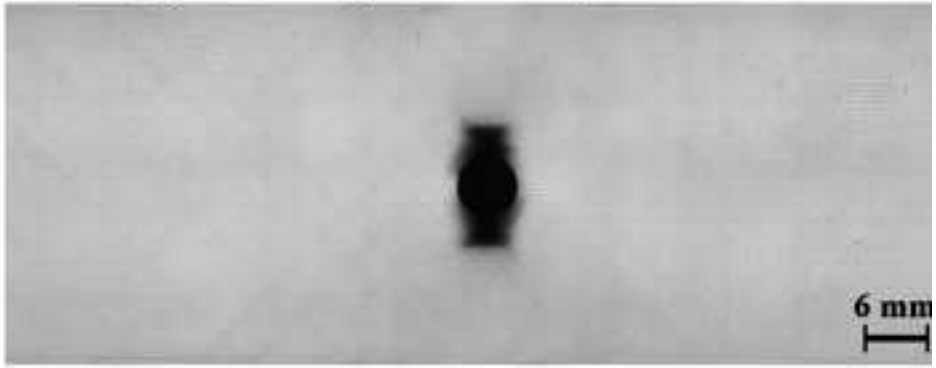

(f) GFRP quasi-isotropic 95% S_{OHT}

Figure 8

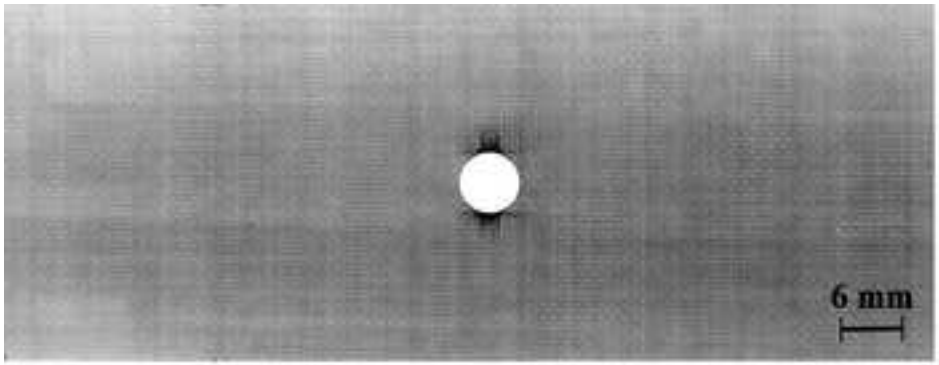

(a) CFRP $[90/0]_{4s}$ 65% S_{OHT}

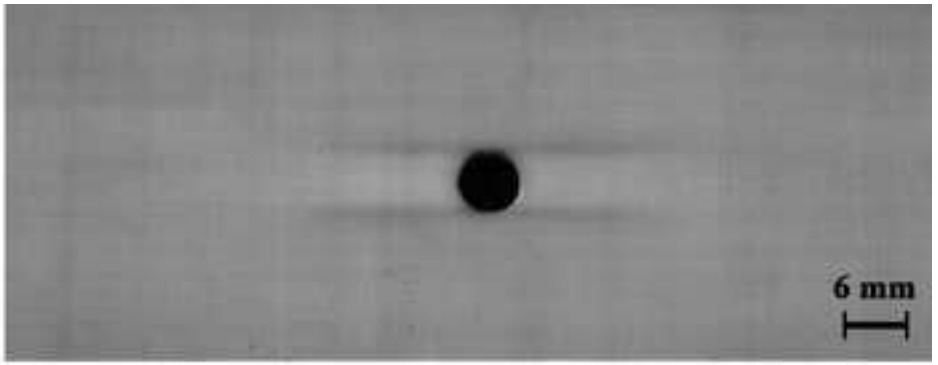

(b) GFRP $[90/0]_{4s}$ 65% S_{OHT}

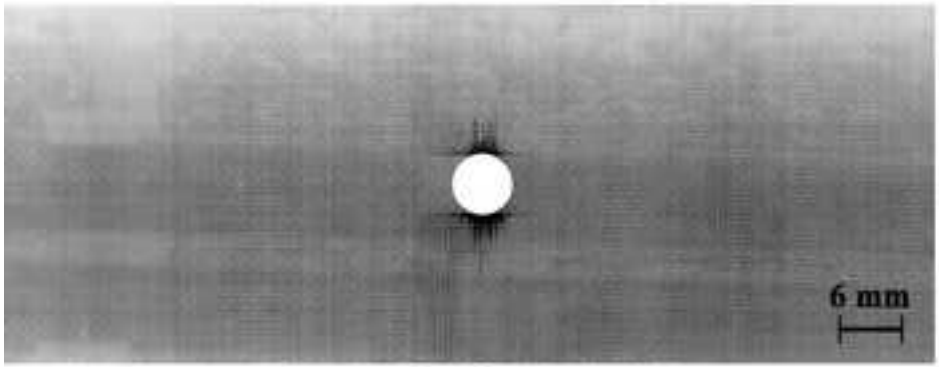

(c) CFRP $[90/0]_{4s}$ 80% S_{OHT}

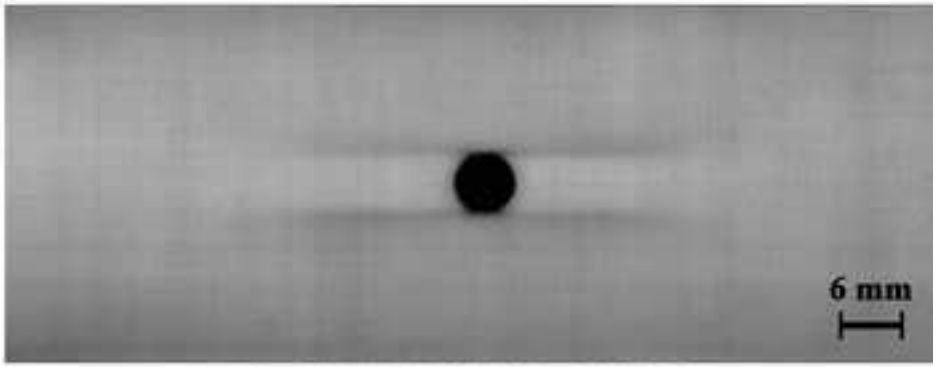

(d) GFRP $[90/0]_{4s}$ 80% S_{OHT}

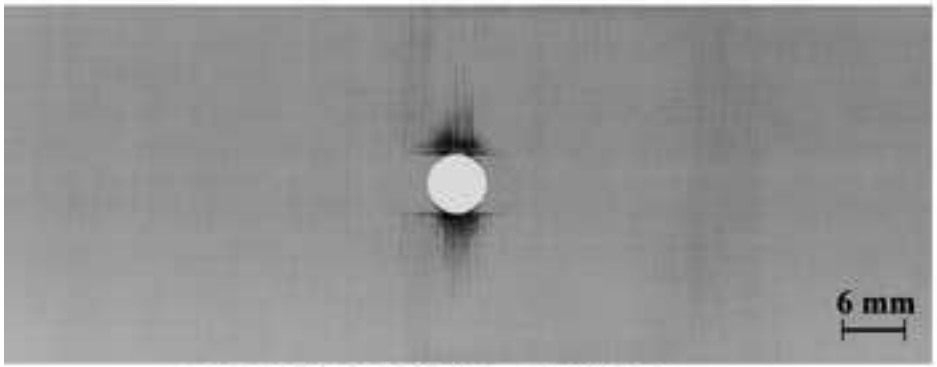

(e) CFRP $[90/0]_{4s}$ 95% S_{OHT}

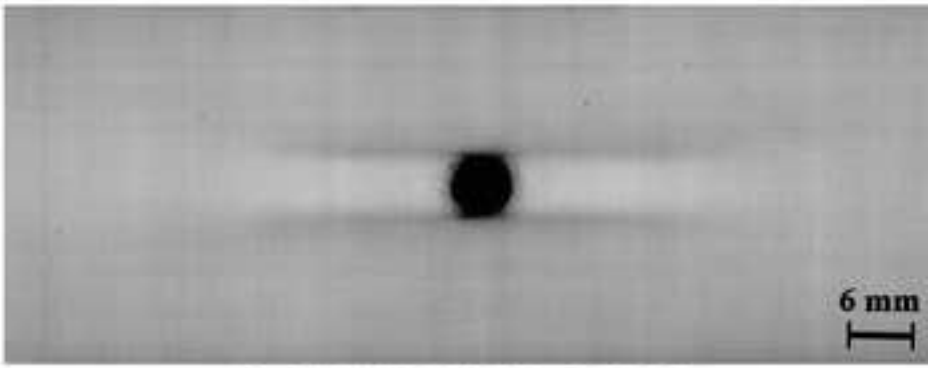

(f) GFRP $[90/0]_{4s}$ 95% S_{OHT}

Figure 9

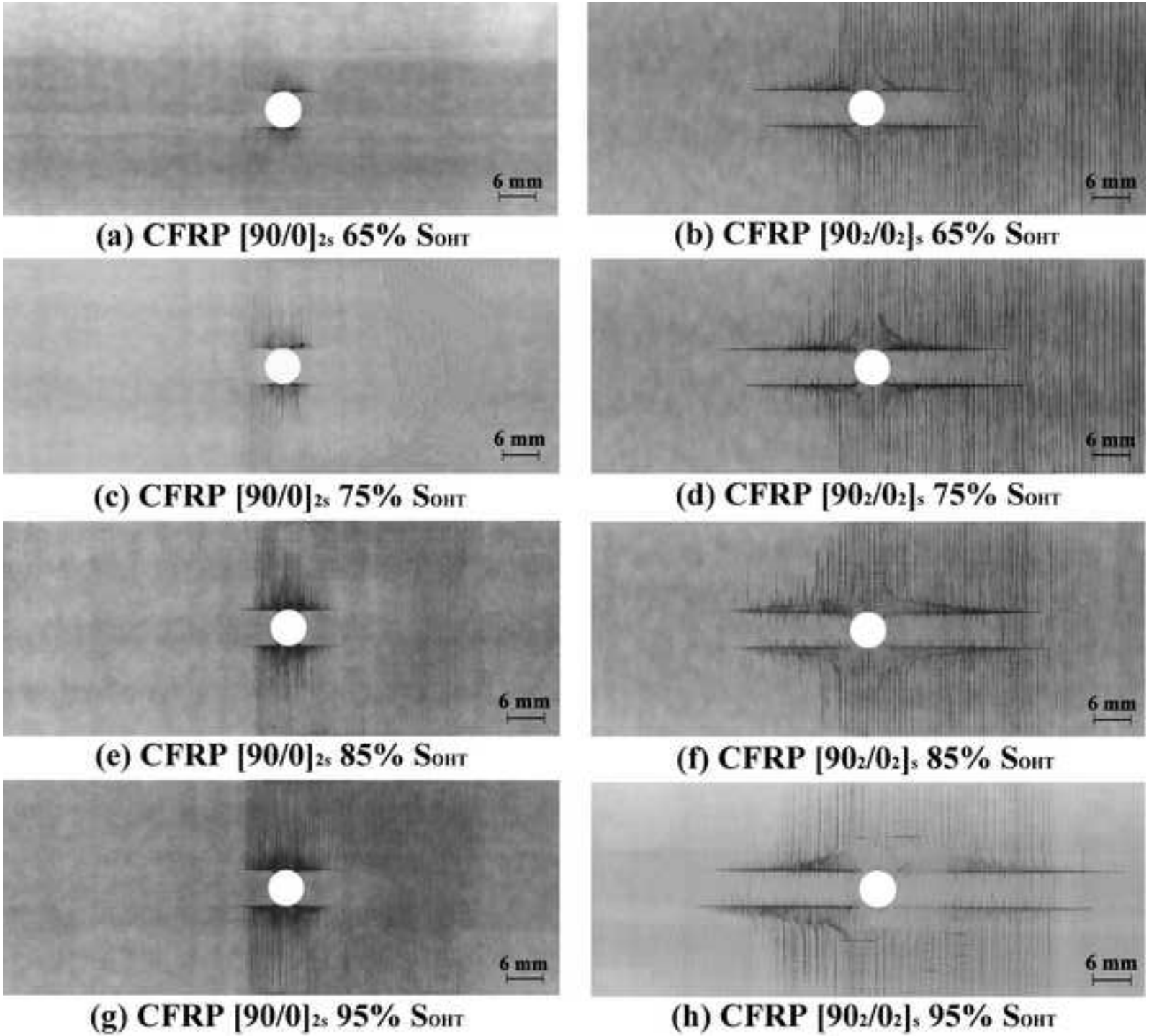
6 mm
(a) CFRP [90/0]2s 65% SOHT
6 mm
(b) CFRP [902/02]s 65% SOHT
6 mm
(c) CFRP [90/0]2s 75% SOHT
6 mm
(d) CFRP [902/02]s 75% SOHT
6 mm
(e) CFRP [90/0]2s 85% SOHT
6 mm
(f) CFRP [902/02]s 85% SOHT
6 mm
(g) CFRP [90/0]2s 95% SOHT
6 mm
(h) CFRP [902/02]s 95% SOHT

Figure 10

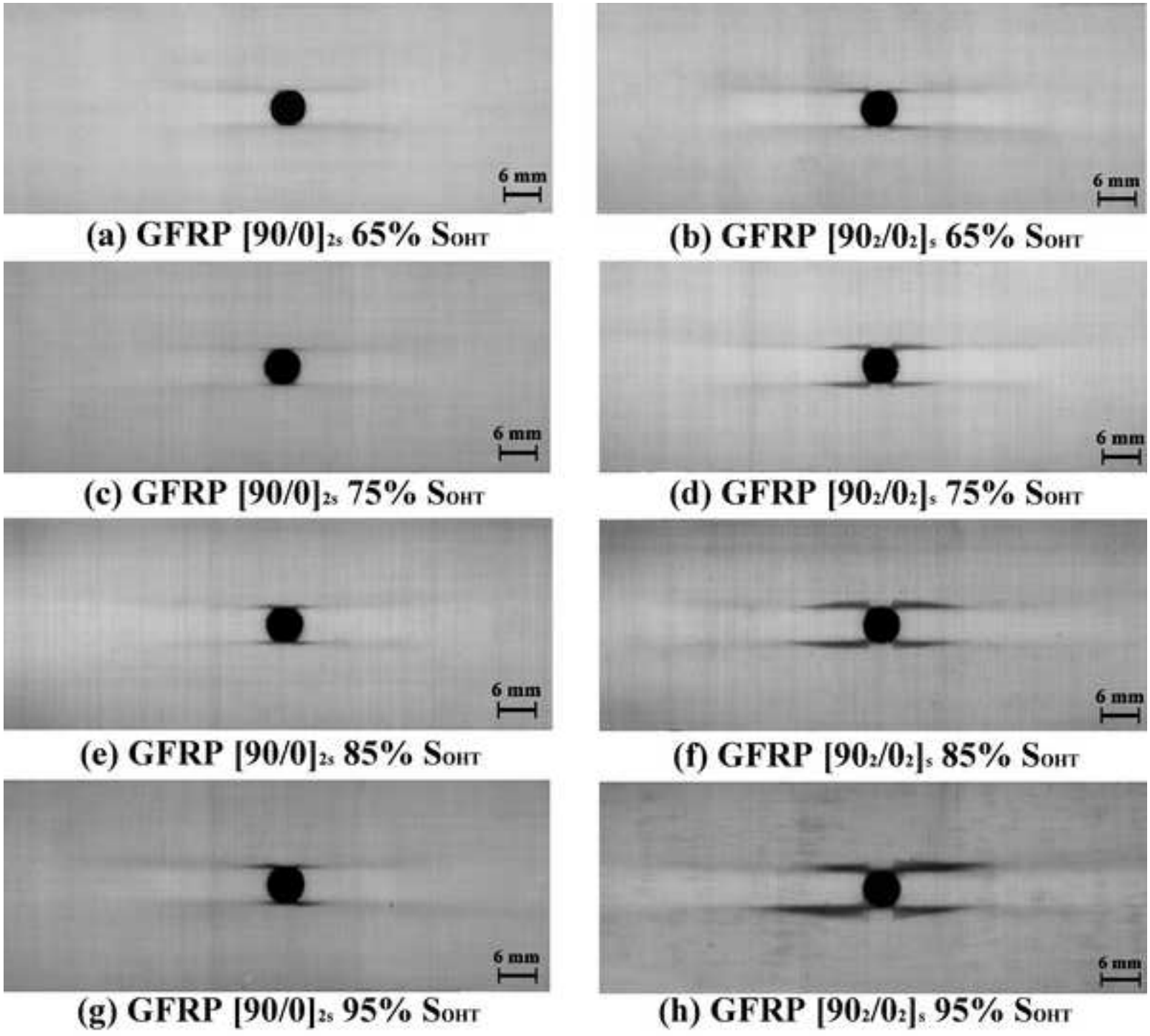
6 mm
(a) GFRP [90/0]2s 65% SOHT
6 mm
(b) GFRP [902/02]s 65% SOHT
6 mm
(c) GFRP [90/0]2s 75% SOHT
6 mm
(d) GFRP [902/02]s 75% SOHT
6 mm
(e) GFRP [90/0]2s 85% SOHT
6 mm
(f) GFRP [902/02]s 85% SOHT
6 mm
(g) GFRP [90/0]2s 95% SOHT
6 mm
(h) GFRP [902/02]s 95% SOHT